Received 3 February 2024, accepted 24 April 2024, date of publication 29 April 2024, date of current version 6 May 2024.
Digital Object Identifier 10.1109/ACCESS.2024.3394931

RESEARCH ARTICLE

A Novel Harmonic Detection Method for Microgrids Based on Variational Mode Decomposition and Improved Harris Hawks Optimization Algorithm

XINCHEN WANG [1], SHAORONG WANG [1], JIAXUAN REN [1], WEIWEI JING [2], MINGMING SHI [2], AND XIAN ZHENG [2]
[1] School of Electrical and Electronic Engineering, Huazhong University of Science and Technology, Wuhan 430074, China
[2] State Grid Jiangsu Electric Power Company Ltd., Nanjing 210024, China
Corresponding author: Xinchen Wang (m202271896@hust.edu.cn)

This work was supported by the State Grid Corporation of China Technologies Program under Grant 5700-202018485A-0-0-00.

ABSTRACT In the pursuit of enhancing harmonic detection precision within microgrids, this paper introduces a pioneering algorithm, VMD-DCHHO-HD, which amalgamates Variational Mode Decomposition (VMD) with an advanced Harris Hawk Optimization algorithm characterized by dynamic opposition-based learning and Cauchy mutation (DCHHO). This study establishes a fitness function based on Shannon entropy, thereby minimizing the Local Minimum Entropy (LME) as the optimization objective for DCHHO. Building upon this, the VMD crucial parameters are efficiently identified using the enhanced HHO algorithm (DCHHO), enabling precise decomposition of complex voltage signals. The proposed method effectively addresses issues commonly encountered in traditional Empirical Mode Decomposition (EMD) during harmonic analysis, such as mode mixing, endpoint effects, and significant errors. Notably, it adeptly captures harmonic components spanning diverse frequencies, offering a nuanced solution to common pitfalls in traditional methodologies. In simulation experiments, VMD-DCHHO-HD showcases remarkable proficiency in extracting microgrid voltage signals, excelling at discerning high-order, low-amplitude harmonic components amid noise. The algorithm's superior precision and heightened reliability, as affirmed by comparative analyses against existing methods, position it as an advanced tool for precise and robust harmonic analysis in microgrid systems.

INDEX TERMS Variational modal decomposition (VMD), harmonic detection, Harris Hawks optimization (HHO) algorithm, function optimization.

I. INTRODUCTION

With the ongoing development of the global economy and society, the escalating environmental challenges associated with fossil fuel usage have propelled a continual rise in demand for various forms of distributed renewable energy sources. The traditional centralized power supply model is increasingly unable to meet the current societal requirements for flexible, environmentally friendly, and efficient electricity transmission. In response to these challenges, microgrid technology has emerged, overcoming the drawbacks of traditional power supply models by offering a flexible power supply mode and effectively enhancing the overall resilience and robustness of the power system [1], [2], [3], [4], [5].

While microgrids present various advantages, it is crucial to tackle the related power quality challenges emerging during their development. On the one hand, the increasing incorporation of nonlinear loads into the grid has become a prevailing trend. On the other hand, the utilization of inverter control technology for diverse distributed energy

The associate editor coordinating the review of this manuscript and approving it for publication was Jenny Mahoney.

sources within microgrids introduces a substantial array of power electronic devices. This presence contributes to distortions in voltage waveforms and an increase in harmonic current levels. Moreover, compared to traditional grid structures, the network framework of microgrids is inherently more fragile, highlighting the significance of harmonic issues [6], [7], [8], [9].

Analyzing harmonic content is not only the starting point for studying harmonic issues but also a crucial basis for formulating harmonic mitigation strategies [10]. Therefore, finding a suitable and efficient algorithm to precisely analyze harmonics in microgrids plays a pivotal role in enhancing the quality of power supply in microgrids. In the quest for effectively extracting features from harmonic signals in microgrids, numerous efficient methods have been proposed, with Fast Fourier Transform (FFT), Wavelet Transform (WT) [11], and Empirical Mode Decomposition (EMD) [12] standing out as chief among them.

FFT [13] is a widely employed and classical tool in time-frequency analysis. However, the traditional FFT falls short in capturing the local properties of signals in the time domain and exhibits reduced effectiveness when dealing with signals characterized by abrupt changes or non-stationarities. Unlike the Fourier Transform, which employs monotonic sine waves, the basis functions used for signal decomposition in WT are diverse, featuring finite durations, abrupt changes in frequency and amplitude, and the ability to scale and shift. On one hand, the flexibility of these basis functions equips the WT to handle abrupt signal changes and perform time-frequency analysis. However, from another perspective, the effectiveness of WT heavily relies on the selection of basis functions. Currently, there is no universally accepted quantifiable method for selecting wavelet bases, and it predominantly depends on the experiential judgment of researchers. While the Wavelet Packet Transform (WPT) [14] surpasses the limitation of the WT by decomposing signals beyond the low-frequency band, it remains powerless in addressing the inherently subjective process of basis function selection. In contrast to WT and WPT, which require the pre-selection of wavelet basis functions, EMD [15] is an adaptive signal analysis method. However, it is imperative to acknowledge the presence of mode mixing and endpoint effect [16]. To address these challenges, a series of refined algorithms based on EMD has emerged, including the Ensemble Empirical Mode Decomposition (EEMD) [17] and the Complementary Ensemble Empirical Mode Decomposition (CEEMD) [18]. However, it is noteworthy that these algorithms incorporate white noise into the signal as a means of mitigating mode mixing, inadvertently leading to an expansion of errors.

In 2014, Konstantin et al. introduced Variational Mode Decomposition (VMD), an adaptive and non-recursive variational mode decomposition method [19]. VMD operates by constructing and solving a variational problem, enabling the decomposition of signals into modes with different central frequencies. Unlike traditional methods like EMD, VMD autonomously determines the number of decomposition modes and adaptively matches optimal central frequencies and finite bandwidths for each mode. VMD effectively separates Intrinsic Mode Functions (IMFs), partitions signals in the frequency domain, and yields efficient decomposed components. It ultimately provides an optimal solution to the variational problem, overcoming issues such as endpoint effects and mode mixing present in methods like EMD. Notably, VMD allows arbitrary specification of parameters like the number of modes; however, imprudent parameter settings can impact decomposition effectiveness in practical applications.

To efficiently and precisely determine the optimal parameters for VMD, maximizing its superiority in harmonic detection, this paper combines an optimization algorithm with VMD. Below are concise descriptions of widely-used optimization algorithms. Compared to traditional gradient-based optimization algorithms, which suffer from both low efficiency and accuracy, Swarm Intelligence (SI) algorithms have proven effective and robust [20], [21]. The Ant Colony Optimization (ACO) [22] algorithm draws inspiration from the foraging behavior of ants to find the optimal path. While robust, the algorithm suffers from slow convergence. Another classic optimization method, the Particle Swarm Optimization (PSO) [23] algorithm, simulates the collective behavior of bird or fish swarms. It excels in requiring minimal parameter configuration and boasts a simple algorithmic structure, but it tends to get stuck in local optima. The Artificial Bee Colony (ABC) [24] algorithm simulates honeybees' foraging behavior, offering high flexibility. However, its processing speed often disappoints when addressing specific problems. Moreover, in recent years, several intriguing optimization algorithms have emerged, including the Grey Wolf Optimization (GWO) [25] algorithm, the Firefly Algorithm (FA) [26] and the Bat Algorithm (BA). While these algorithms offer distinct advantages, they share common limitations, including challenges in handling complex scenarios and issues related to global exploration.

In 2019, the Harris Hawk Optimization (HHO) algorithm was introduced by the Iranian scholar Heidari et al. [27]. This nature-inspired swarm intelligence approach, emulating the hunting behavior of Harris hawks, is relatively straightforward compared to other optimization algorithms. The HHO algorithm adopts a parallel search strategy, significantly accelerating the convergence speed. Additionally, the HHO algorithm introduces competitive and search mechanisms, allowing for adaptive adjustment of algorithm parameters, showcasing high adaptability and robustness. Leveraging these advantages, this paper opts to employ the HHO to optimize the VMD. Furthermore, additional enhancements to the HHO algorithm are discussed later in the paper, improving algorithm performance.

This paper delves into the harmonic analysis of microgrids, introducing the innovative VMD-DCHHO-HD algorithm to overcome existing method limitations. This novel harmonic detection algorithm effectively tackles the parameter selection challenge in VMD. Importantly, it excels in extracting harmonic signal characteristics within microgrid scenarios, surpassing the performance of previous mainstream algorithms and pushing the boundaries of the field. The primary contributions of the paper can be summarized as follows:

1) Introduced an enhanced algorithm, DCHHO, based on Harris Hawk Optimization, aiming to comprehensively rectify its deficiencies and meticulously adapt it for the determination of optimal algorithm parameters. The detailed optimization strategy is outlined as follows:
   - Introduced Cauchy mutation to enable the HHO algorithm to escape local optima during the optimization process.
   - Introduced dynamic opposition-based learning to enhance the optimization efficiency of the HHO algorithm.
2) Incorporated DCHHO into VMD, adeptly identifying the optimal combination of crucial parameters for VMD. This integration resulted in the demonstration of superior modal decomposition, highlighting its effectiveness in harmonic detection within microgrid scenarios.
3) Simulated a microgrid system in MATLAB, conducted analysis and comparative experiments using the simulated voltage signals, demonstrating the effectiveness and engineering applicability of the proposed novel algorithm.

II. PRINCIPLES OF MATHEMATICS

A. VMD

The VMD decomposition can be conceptually framed as an optimization process for solving the following constrained variational problem [28], as illustrated in (1).

$$\left\{\sum_k \left\| \partial_t \left[\left(\delta(t) + \frac{j}{\pi t} \right) * u_k(t) \right] e^{-j\omega_k t} \right\|^2 \right\} \quad s.t. \quad \sum_k u_k = f \tag{1}$$

where, $\{u_k\} = \{u_1, \cdots, u_k\}$ symbolizes the decomposed Intrinsic Mode Function (IMF) component, while $\{\omega_k\} = \{\omega_1, \cdots, \omega_k\}$ represents the central frequency of each constituent part. Here, $\delta(t)$ denotes the Dirac distribution, and the symbol $*$ corresponds to the convolution operator.

By introducing the Lagrange multiplier operator λ, transforming the constrained variational problem into an unconstrained one. The augmented Lagrange expression is obtained as (2):

$$\begin{aligned} &L(\{u_k\}, \{\omega_k\}, \lambda) \\ &= \alpha \sum_k \left\| \partial_t \left[\left(\delta(t) + \frac{j}{\pi t} \right) * u_k(t) \right] e^{-j\omega_k t} \right\|_2^2 \\ &+ \left\| f(t) - \sum_k u_k(t) \right\|_2^2 + \left\langle \lambda(t), f(t) - \sum_k u_k(t) \right\rangle \end{aligned} \tag{2}$$

where, α serves as the quadratic penalty factor designed to mitigate the interference of Gaussian noise. Subsequently, utilizing the Alternating Direction Method of Multipliers (ADMM), each component and its corresponding central frequency are iteratively updated. Ultimately, this process yields the saddle point of the unconstrained model, representing the optimal solution to the original problem. The specific steps and formulas are described as follows.

After initializing parameters $\hat{u}_k^1, \omega_k^1, \lambda^1$, iterative updates are systematically carried out in accordance with (3), (4) and (5).

$$\hat{u}_k^{n+1}(\omega) = \frac{\hat{s}(\omega) - \sum_{i \neq k} \hat{u}_i(\omega) + \hat{\tau}(\omega)/2}{1 + 2\alpha(\omega - \omega_k)^2} \tag{3}$$

$$\omega_k^{n+1} = \frac{\int_0^\infty \omega \left| \hat{u}_k^{n+1}(\omega) \right|^2 d\omega}{\int_0^\infty \left| \hat{u}_k^{n+1}(\omega) \right|^2 d\omega} \tag{4}$$

$$\hat{\lambda}^{n+1}(\omega) = \hat{\lambda}^n(\omega) + \gamma \left(\hat{f}(\omega) - \sum_k \hat{u}_k^{n+1}(\omega) \right) \tag{5}$$

Repeating the steps until the iterative stopping condition $\sum_k \left\| \hat{u}_k^{n+1} - \hat{u}_k^n \right\|_2^2 / \left\| \hat{u}_k^n \right\|_2^2 < \varepsilon$.

B. HHO

The Harris Hawk Optimization (HHO) algorithm is renowned for robust global search and strong optimization performance, organized into three distinct stages.

1) EXPLORATION PHASE

In this phase, the Harris hawks utilize two strategies for the random search of prey within the spatial range $[lb, ub]$. Throughout iterations, the positions undergo updates guided by q, as (6):

$$X(t+1) = \begin{cases} X_{rand} - r_1 |X_{rand}(t) - 2r_2 X(t)|, & q \geq 0.5 \\ (X_{rabbit}(t) - X_m(t)) - r_3 (lb + r_4(ub - lb)), & q < 0.5 \end{cases} \tag{6}$$

where $X_{rabbit}(t)$ represents the prey's position, $X(t)$ denotes the Harris hawk's position, $X_{rand}(t)$ signifies the randomly selected individual's position, $X_m(t)$ is the mean position of individuals, q, r_1, r_2, r_3, r_4 are random numbers within the range (0,1).

2) TRANSITION PHASE

In this phase, the escape energy equation for prey is defined, as illustrated in (7), facilitating a suitable transition between exploration and exploitation through the utilization of (7).

$$E = 2E_0 \left(1 - \frac{t}{T} \right) \tag{7}$$

where E represents the escape energy of the prey, with E_0 being the initial energy level. When $|E| \geq 1$, the Harris Hawk algorithm conducts global exploration. Once $|E| < 1$, the algorithm transitions into the local exploitation phase.

3) EXPLOITATION PHASE

In this phase, the algorithm employs four strategies to simulate attacking behavior. Tab.1 outlines these strategies employed by Harris hawks for capturing prey under different conditions, providing a detailed description of their respective position iteration equations.

TABLE 1. The harris hawk position iteration equation under different conditions.

Approach	Conditions	The Harris hawk position iteration equation
Soft besiege	$\begin{cases}\lvert E\rvert \ge 0.5\\ \lambda \ge 0.5\end{cases}$	$X(t+1) = \Delta X(t) - E\lvert JX_{rabbit}(t) - X(t)\rvert$ $\Delta X(t) = X_{rabbit}(t) - X(t)$
Hard besiege	$\begin{cases}\lvert E\rvert < 0.5\\ \lambda \ge 0.5\end{cases}$	$X(t+1) = X_{rabbit}(t) - E\lvert \Delta X(t)\rvert$
soft besiege with progressive rapid dives	$\begin{cases}\lvert E\rvert < 0.5\\ \lambda < 0.5\end{cases}$	$X(t+1) = \begin{cases}Y, F(Y) < F(X(t))\\ Z, F(Z) < F(X(t))\end{cases}$ $Y: X_{rabbit}(t) - E\lvert JX_{rabbit}(t) - X(t)\rvert$ $Z: Y + S \times LF(Dim)$
hard besiege with progressive rapid dives	$\begin{cases}\lvert E\rvert \ge 0.5\\ \lambda < 0.5\end{cases}$	$X(t+1) = \begin{cases}Y, F(Y) < F(X(t))\\ Z, F(Z) < F(X(t))\end{cases}$ $Y: X_{rabbit}(t) - E\lvert JX_{rabbit}(t) - X_m(t)\rvert$ $Z: Y + S \times LF(Dim)$

III. ALGORITHMIC IMPROVEMENT MOTIVATIONS

While VMD and modal decomposition algorithms like EMD, EEMD, and CEEMD share a common purpose, they exhibit fundamental differences. VMD, in contrast to EMD and its derivatives, offers the advantage of pre-specifying the number of modes and the penalty parameter α. However, due to the intricate nature of real-world signals, improper settings for parameters k and α can potentially negate this advantage. An excessively large k may result in over-decomposition problem, while an excessively small one may lead to under-decomposition problem. Similarly, an overly large α could cause the loss of frequency band information, while an overly small α may result in information redundancy [29], [30].

Presently, the widely adopted method involves using the central frequency observation approach to determine suitable values for k and α. However, this method is highly subjective, diminishing the VMD algorithm's fault tolerance and providing insufficient determination of the penalty parameter α. Consequently, the selection of an optimal parameter combination is a critical and challenging aspect in applying the VMD algorithm for harmonic information extraction.

In light of this, the study seamlessly integrates optimization algorithms with VMD to precisely define its critical parameters, effectively capitalizing on its strengths and mitigating limitations for optimal performance in modal decomposition. To better achieve this goal, this paper enhances the Harris Hawk Optimization (HHO) algorithm, significantly addressing its susceptibility to local optima and thereby improving both algorithm accuracy and optimization efficiency.

The overall system block diagram of the proposed VMD-DCHHO-HD for microgrid harmonic detection is illustrated in Fig.1.

IV. A NOVEL HARMONIC DETECTION METHOD BASED ON VMD AND IMPROVED HHO ALGORITHM (VMD-DCHHO-HD)

A. OPTIMIZATION OF THE HHO ALGORITHM

The Harris Hawk Optimization (HHO) algorithm, drawing inspiration from the hunting behavior of Harris hawks, is a nature-inspired swarm intelligence algorithm recognized for its robust global search capabilities and optimization performance. However, it encounters challenges such as susceptibility to local optima and low convergence accuracy.

This study enhances the HHO algorithm by introducing the Cauchy operator and the dynamic opposition-based learning strategy. The resulting refined algorithm exhibits improved robustness and optimization performance, particularly proving beneficial for addressing complex harmonic problems.

1) CAUCHY MUTATION

To alleviate the susceptibility of HHO algorithm to local optima, drawing inspiration from the work referenced in [31] and [32], this study incorporates optimization by integrating the Cauchy distribution function. Harnessing the unique attributes of the Cauchy distribution function, characterized by a smaller peak at the origin and an extended distribution at both ends, the inclusion of the Cauchy operator in the HHO algorithm amplifies mutation effects at both ends during optimization, yielding enhanced performance.

$$f(x) = \frac{1}{\pi}\left(\frac{1}{x^2+1}\right) \tag{8}$$

The update of the global optimum in each iteration of HHO is determined using the standard Cauchy distribution function (8), represented by (9). Leveraging the properties of the Cauchy function, characterized by a moderate peak, effectively reduces the exploration time spent by Harris hawks in local intervals. Notably, the gradual decline at both ends of the Cauchy function mitigates the algorithm's constraint force on local extreme points, facilitating escape from local optima.

$$X_{new\_best} = X_{best} + X_{best} \times Cauchy(0, 1) \tag{9}$$

2) DYNAMIC OPPOSITION-BASED LEARNING STRATEGY

Taking inspiration from prior studies [32], [33], this research integrates the dynamic opposition-based learning strategy to improve the efficiency of acquiring optimal solutions.

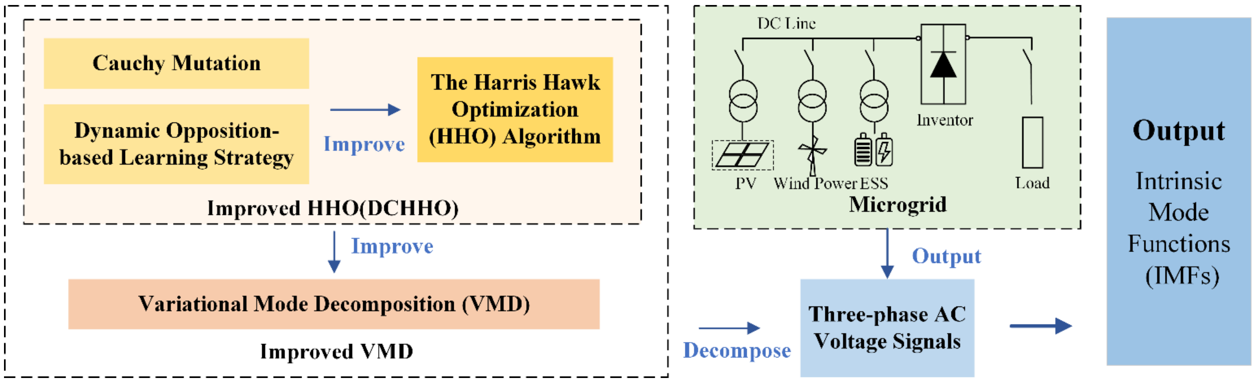

FIGURE 1. Block diagram of the harmonic detection system.

The core principle of opposition-based learning entails generating a solution derived from the current one. Simultaneous searches are conducted at the present position and its opposite counterpart, heightening the probability of attaining superior solutions. The dynamic opposition-based learning introduces a variable, denoted as r, which undergoes nonlinear evolution with each iteration, more effectively steering the generation of reverse solutions. This relationship is mathematically expressed in (10) and (11).

$$\tilde{X}_i(t) = lb + ub - rX_i(t) \tag{10}$$

$$r = \sin\left(\frac{t}{T}\right) \tag{11}$$

In the search space $[lb, ub]$, where t represents the iteration time, $X_i(t)$ denotes the position of individual i at time t, $\tilde{X}_i(t)$ represents its corresponding reverse solution, and r is the dynamic coefficient.

B. CHOOSING THE FITNESS FUNCTION

In the process of optimizing the important parameters for the VMD algorithm using the enhanced the Harris Hawk Optimization algorithm, it is crucial to define a fitness function [34], [35]. This fitness function involves continuous calculation and comparison of fitness values, leading to the updating of the optimal position.

Drawing inspiration from the literature [36], this study employs Shannon entropy to assess the sparsity characteristics of the signal. The magnitude of entropy reflects the uniformity of the probability distribution, with the highest entropy value associated with the most uncertain probability distribution [37]. Following this principle, the envelope signal obtained through signal demodulation undergoes processing into a probability distribution sequence p_j. The resulting entropy value E_p calculated from this sequence effectively captures the sparsity characteristics of the original signal.

For each individual's position in the HHO algorithm, the condition involves obtaining the envelope entropy values of all IMF components after VMD processing. Among these values, the minimum one is defined as the Local Minimum Entropy (LME). Based on the definition of entropy, the less noise contained in the IMF components, the more characteristic information is present, and the signal exhibits stronger sparsity characteristics, resulting in smaller envelope entropy values. Therefore, this study minimizes the Local Minimum Entropy value as the optimization objective, aiming to optimize the values of k and α, as mathematically formulated in (12).

$$L = \min E_{p\min}^{IMF} \tag{12}$$

C. SPECIFIC STEPS OF THE VMD-DCHHO-HD

The process diagram of the enhanced harmonic analysis algorithm, VMD-DCHHO-HD, resulting from the aforementioned optimization innovations, is illustrated in Fig.2.

The specific steps of execution are outlined below:

Step 1: Initialization of the parameters to be determined in the VMD algorithm, minimizing the local minimum entropy as the optimization objective, and determining the fitness function, as shown in (12).

Step 2: Initialize the whole population with parameter combinations $[k\ \alpha]$ as individual positions, calculate the fitness value for each individual, and determine the current optimal individual.

Step 3: Calculate the initial energy and escape energy for each individual, based on which determine whether the Harris hawk individual is in the exploration phase or exploitation phase. Continuously update individual positions accordingly.

Step 4: Apply Cauchy mutation to the optimal solution of individuals in the capturing phase according to (9).

Step 5: Implement the dynamic opposition-based learning operations on all individuals using (10). Combine the newly acquired population with the original population, employing the greedy strategy to select the top N individuals with the highest fitness values for the new population.

Step 6: Continuously update the positions of Harris's hawk and the global optimal solution.

Step 7: Check for convergence: if the maximum number of iterations is not reached, continue the iterative process; otherwise, report the final global optimal solution $[k_{best}\ \alpha_{best}]$ and its corresponding best fitness value.

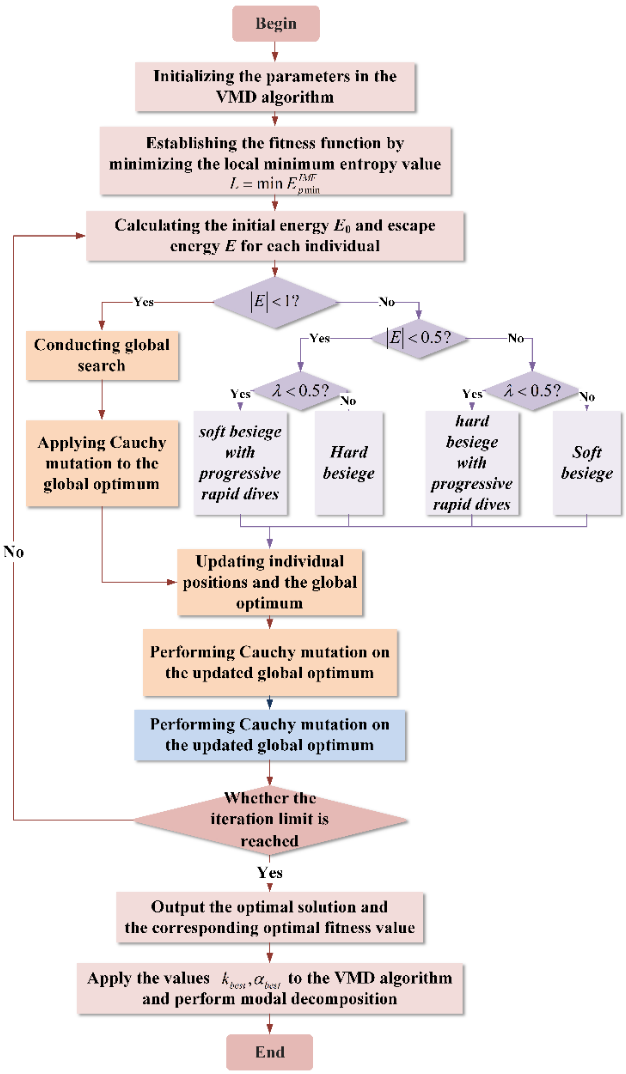

FIGURE 2. The procedure for harmonic detection based on the VMD-DCHHO-HD algorithm.

Step 8: Apply the values k_{best}, α_{best} to the VMD algorithm and perform modal decomposition.

V. SIMULATIONS AND RESULTS

A. MICROGRID VOLTAGE SIGNAL SIMULATION

To evaluate the practical applicability of the proposed algorithm, this paper implemented a three-phase AC circuit using MATLAB. The circuit configuration, illustrated in Fig.3, simulates a DC Microgrid for Wind and Solar Power Integration, demonstrating significant growth potential and versatile applications. The microgrid includes components such as Wind Turbine (WT) system, Photovoltaic (PV) system, and Supercapacitor Energy Storage (SCES) system. These components are connected to the DC bus using a DC-DC converter. The transformed and filtered AC power is then supplied to loads through the inverter [38], [39], [40], [41], [42]. Due to constraints on the length of this paper, a detailed discussion of each module's structure is beyond the scope.

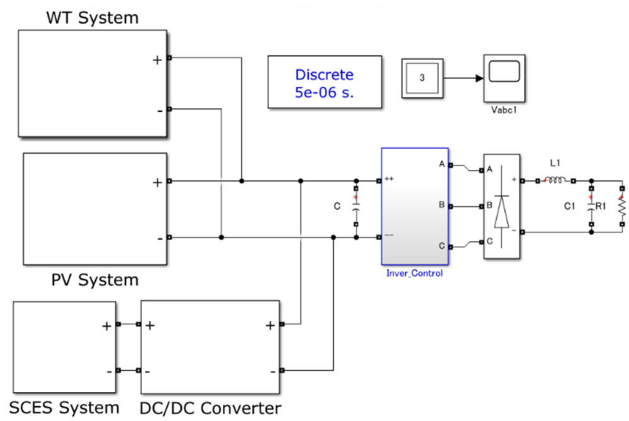

FIGURE 3. Simulation of DC microgrid for wind and solar power integration system.

In traditional power systems, sources of pollution mostly arise from harmonics generated internally during the processes of generation, transmission, and distribution processes, as well as the connection of nonlinear loads such as inverters, rectifiers, etc. In contrast to traditional power systems, microgrid systems on the source side incorporate numerous power electronic devices, further contributing to the degradation of power quality. Therefore, harmonic management is a crucial technical focus in microgrid planning.

1) SIMULATION PARAMETERS

To maximize the electric power generated from the wind, the Wind Turbine (WT) system described in this paper is designed based on the traditional Maximum Power Point Tracking (MPPT) control strategy [43], [44]. The system features a direct-drive structure, where there is no transmission system between the rotor and the generator, ensuring higher transmission efficiency. Additionally, a Buck-Boost converter is integrated before the load to address the low amplitude of the AC voltage output. During operation, the system initiates with a pitch angle set to 0 and a wind speed of 8 m/s. Tuning is performed to validate the system's ability to swiftly attain the Maximum Power Point shortly after the commencement of operation.

The PV system in this study employs the constant-step Perturbation and Observation (P&O) MPPT algorithm [45]. Similarly, a Buck-Boost converter is introduced between the output and the load. The system operates under a set solar irradiance of $1200W/cm^2$, showcasing commendable response speed following tuning [46].

The energy storage system utilizes a supercapacitor to output a vector containing measurement signals. Facilitated by a bidirectional Buck-Boost converter, the energy storage system achieves bidirectional charging and discharging control of the supercapacitor. Integration of a Proportional-Integral (PI) control system ensures the stable voltage and current operation of the energy storage system [47], [48].

2) SIMULATION RESULTS OF THE VOLTAGE SIGNAL

The load side has $R = 0.02\Omega$ and $L = 0.1$mH, and a 5 kW AC load is connected before the system is operated. The output three-phase AC voltage signals are shown in Fig.4.

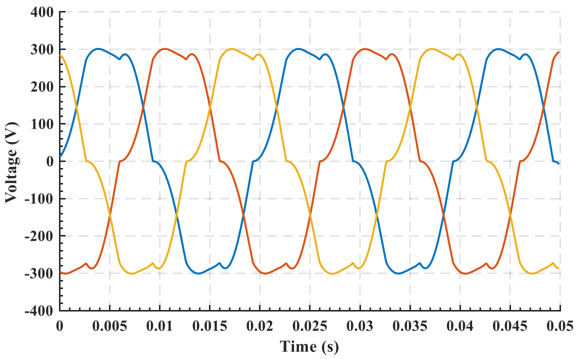

FIGURE 4. Simulation results of three-phase AC voltage signals at the load side of the microgrid.

From Fig.4, it can be observed that the simulated voltage signals of the microgrid contain numerous harmonic components with unknown frequencies and amplitudes. To facilitate further analysis, the next step will involve harmonic detection on the single-phase voltage signals extracted from these signals.

B. ANALYSIS OF THE VMD PERFORMANCE OPTIMIZED BY DCHHO

Setting the maximum iteration count to 30, using the minimum envelope entropy as the fitness function, the DCHHO algorithm efficiently obtains the optimal solution for the important parameters of VMD. The optimization process is illustrated in Fig.5.

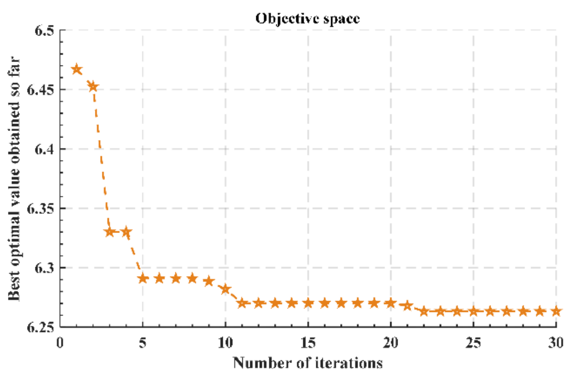

FIGURE 5. The iterative process of utilizing the DCHHO algorithm to find the optimal parameters for VMD.

In Fig.5, it is evident that, with an increase in the number of iterations, the optimal combination of $[k\ \alpha]$ stabilizes at [9 669]. This indicates that the optimal number of modes obtained through DCHHO is 9, with the optimal penalty parameter being 669. The corresponding optimal fitness value for this combination is 6.2633. The decomposition result of VMD-DCHHO-HD based on this optimal parameter set is illustrated in Fig.6.

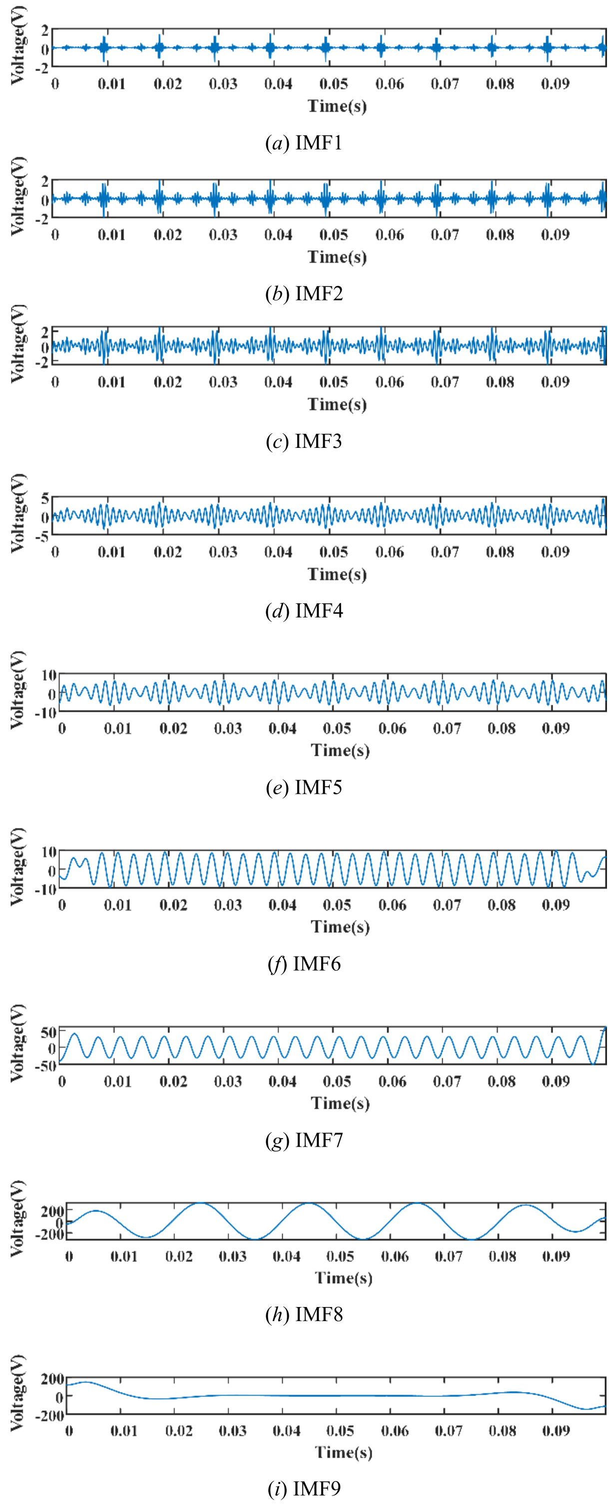

FIGURE 6. Results of modal decomposition of microgrid output voltage signal using VMD-DCHHO-HD algorithm.

Observing the IMFs depicted in Fig. 6, it is evident that VMD-DCHHO-HD excels in achieving a remarkable modal decomposition for the intricate voltage signals in the microgrid. The algorithm precisely isolates harmonic signals spanning various frequencies, effectively suppressing modal aliasing and thereby facilitating a simplified yet comprehensive harmonic analysis. To underscore the superior performance of our novel harmonic detection algorithm, the following section conducts a comparative analysis with several widely adopted harmonic detection algorithms.

C. COMPARISONS AND ANALYSIS OF EXPERIMENTAL RESULTS

Building upon the research content and objectives outlined in the preceding section, this segment employs various decomposition algorithms—EMD, EEMD, CEEMD, and VMD-DCHHO-HD—to analyze the steady-state single-phase voltage signals obtained from the simulation in Section A of Phase V. The ensuing discussion involves a comparative analysis of the effectiveness of these algorithms. Due to constraints in space, a detailed presentation of the IMFs obtained by each algorithm is omitted. Given that the spectrogram provides ample information and visual clarity, this paper will integrate the spectrogram along with metrics such as Mutual Information (MI) and Root Mean Square Error (RMSE) to illustrate the effects of modal decomposition.

Fig.7 illustrates the spectrograms of decomposition results obtained by each algorithm. Based on Fig.7 (*a*), it is evident that the EMD algorithm, applied to the voltage signal with complex harmonic information obtained from the microgrid simulation in this study, adaptively decomposes it into five IMFs. However, the effectiveness of this decomposition is suboptimal. The spectrogram clearly indicates a substantial loss of high-frequency information after signal decomposition, retaining only harmonic signals below $10f_0$ and the fundamental frequency signal. Furthermore, the IMFs exhibit pronounced mode mixing and noticeable endpoint effects, highlighting the subpar performance of EMD in harmonic analysis for the simulated voltage signal.

As depicted in Fig.7 (*b*) and (*c*), the enhanced versions of EMD, namely EEMD and CEEMD, exhibit improvements in mitigating endpoint effects and reducing the loss of high-frequency signals compared to the original EMD. However, despite addressing these issues, both modified algorithms still suffer from mode mixing problems. Additionally, the improvements come at a cost, as these enhanced algorithms introduce white noise into the decomposition process. While this helps suppress mode mixing, it simultaneously results in the generation of numerous false components, leading to an increase in errors.

In comparison to EMD, EEMD, and CEEMD, Fig.7(*d*) distinctly reveals the superior performance of VMD-DCHHO-HD in resolving mode mixing and endpoint effects. This is particularly notable for harmonics within the $20f_0$ range, including $5f_0$, $7f_0$, $11f_0$, $13f_0$, $17f_0$, and $19f_0$, where the algorithm exhibits exceptional separation capabilities.

To further elevate the precision of performance evaluation in harmonic detection, this study introduces evaluation metrics, including Mutual Information (MI) and Root Mean Square Error (RMSE). Subsequently, a comparative table is provided for a systematic analysis and comparison of these algorithm.

Mutual Information (MI) serves as a non-parametric and non-linear metric in information theory, offering a precise quantification of the correlation between two random variables [49], [50]. In contrast to traditional correlation coefficient methods, MI accurately reflects the coupling degree between IMFs. Combining the analysis of MI and spectrograms provides a clearer and more intuitive understanding of an algorithm's ability to address mode mixing. MI is defined by (13).

$$\mathrm{MI}(\mathrm{y}_i,\mathrm{y}_j) = \mathrm{E}\left[\log\left(\frac{p^{y_i,y_j}(y_i,y_j)}{p^{y_i}(y_i)p^{y_j}(y_j)}\right)\right] \tag{13}$$

where y_i represents the signal amplitude corresponding to IMF_i, y_j represents the signal amplitude corresponding to IMF_j, $p^{yi,yj}(y_i, y_j)$ is the joint probability density function, $p^{yi}(y_i)$ and $p^{yj}(y_j)$ are the marginal probability density functions.

Root Mean Square Error (RMSE) effectively reflects the difference between the reconstructed signal and the initial signal. A larger RMSE indicates a greater amount of error introduced by the harmonic detection algorithm during the modal decomposition process. RMSE is defined by (14).

$$RMSE(\hat{y}, y) = \sqrt{\frac{1}{N}\sum_{i=1}^{n}(\hat{y}-y)^2} \tag{14}$$

where $\hat{y}$ represents the amplitude of the reconstructed signal, y represents the amplitude of the initial signal and N represents the number of sampling points.

Additionally, as the assessment of endpoint effects in the initial signal decomposition process cannot be captured by a specific metric, we will directly summarize based on spectrograms. The findings will be presented and compared in Tab.2.

Analyzing the metrics in Tab.2, it is evident that the RMSE corresponding to VMD-DCHHO-HD is 0.6998, significantly smaller than the other algorithms. This indicates

TABLE 2. Comparison of multiple metrics.

Indicators	EMD	EEMD	CEEMD	VMD-DCHHO-HD
RMSE	5.4694	4.3877	1.9555	0.6998
MI between IMFs	$\mathrm{IMF}_{1\text{-}2}$:0.2457 $\mathrm{IMF}_{2\text{-}3}$:0.3875 $\mathrm{IMF}_{3\text{-}4}$:0.5650 $\mathrm{IMF}_{4\text{-}5}$:0.6706	$\mathrm{IMF}_{1\text{-}2}$:0.2740 $\mathrm{IMF}_{2\text{-}3}$:0.1351 $\mathrm{IMF}_{3\text{-}4}$:0.2517 $\mathrm{IMF}_{4\text{-}5}$:0.3862	$\mathrm{IMF}_{1\text{-}2}$:0.2228 $\mathrm{IMF}_{2\text{-}3}$:0.2047 $\mathrm{IMF}_{3\text{-}4}$:0.3623 $\mathrm{IMF}_{4\text{-}5}$:0.2030 $\mathrm{IMF}_{5\text{-}6}$:0.2690	$\mathrm{IMF}_{1\text{-}2}$:0.0271 $\mathrm{IMF}_{2\text{-}3}$:0.0754 $\mathrm{IMF}_{3\text{-}4}$:0.0117 $\mathrm{IMF}_{4\text{-}5}$:0.0068 $\mathrm{IMF}_{5\text{-}6}$:0.0533 $\mathrm{IMF}_{6\text{-}7}$:0.2771 $\mathrm{IMF}_{7\text{-}8}$:0.1219 $\mathrm{IMF}_{8\text{-}9}$:0.0998
Occurrence of Endpoint Effects (Yes/No)	Yes	No	No	No

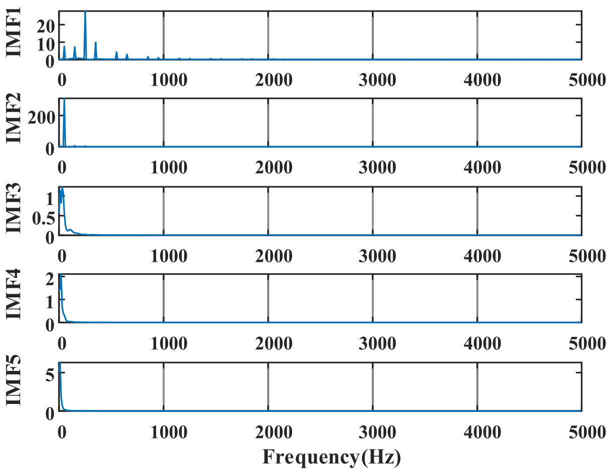

(*a*) Spectrogram illustrating the results obtained from the decomposition of the initial voltage signal using EMD.

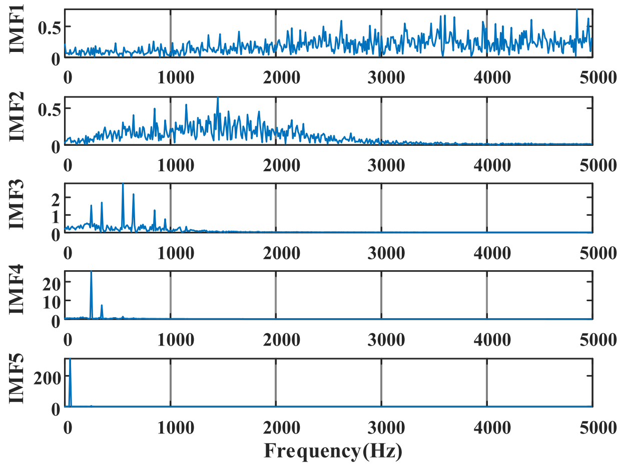

(*b*) Spectrogram illustrating the results obtained from the decomposition of the initial voltage signal using EEMD.

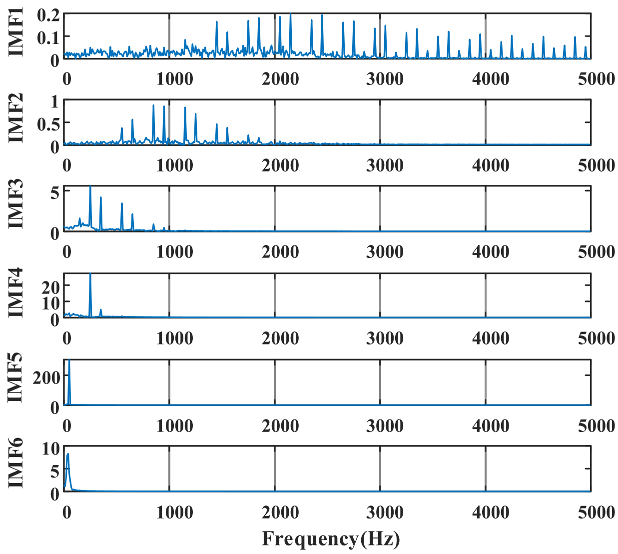

(*c*) Spectrogram illustrating the results obtained from the decomposition of the initial voltage signal using CEEMD.

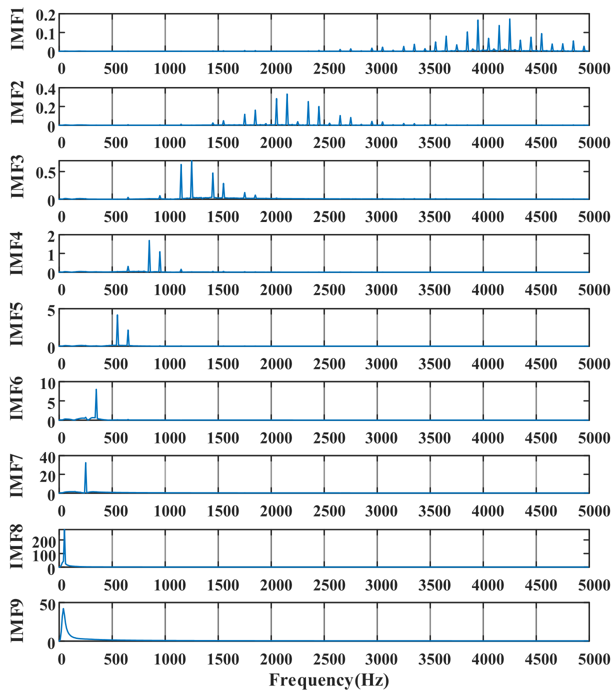

(*d*) Spectrogram illustrating the results obtained from the decomposition of the initial voltage signal using VMD-DCHHO-HD.

FIGURE 7. Spectrograms of decomposition results for each algorithm.

that the algorithm introduces minimal error and demonstrates high precision. Furthermore, the MI between adjacent IMFs obtained through VMD-DCHHO-HD is closest to 0. Combining this with the spectrogram in Fig.7, it is evident that the proposed method effectively eliminates redundant components in each IMF, successfully overcoming the mode-mixing problem. Additionally, the algorithm almost perfectly eliminates endpoint effects.

In conclusion, the algorithm exhibits outstanding performance in balancing decomposition effectiveness and precision. It outperforms traditional harmonic detection algorithms in various performance indicators.

VI. CONCLUSION

This paper presents VMD-DCHHO-HD, a novel microgrid harmonic detection algorithm integrating an improved HHO algorithm with VMD. Comparative analysis with well-known algorithms, such as EMD, EEMD, and CEEMD, highlights the superior performance of VMD-DCHHO-HD in overcoming endpoint effects and mode-mixing issues, showcasing remarkable precision. The algorithm excels in extracting microgrid fundamental signals, accurately capturing high-order, low-amplitude harmonics amid noise. Its effectiveness positions VMD-DCHHO-HD as a superior choice for microgrid harmonic detection. Our future research will explore harmonic source identification and suppression strategies using this innovative detection method.

REFERENCES

[1] R. Keypour, B. Adineh, M. H. Khooban, and F. Blaabjerg, "A new population-based optimization method for online minimization of voltage harmonics in islanded microgrids," *IEEE Trans. Circuits Syst. II, Exp. Briefs*, vol. 67, no. 6, pp. 1084–1088, Jun. 2020, doi: 10.1109/TCSII.2019.2927208.

[2] A. Micallef, M. Apap, C. Spiteri-Staines, and J. M. Guerrero, "Mitigation of harmonics in grid-connected and islanded microgrids via virtual admittances and impedances," *IEEE Trans. Smart Grid*, vol. 8, no. 2, pp. 651–661, Mar. 2017, doi: 10.1109/TSG.2015.2497409.

[3] Z. Zhao, J. Zhang, B. Yan, R. Cheng, C. S. Lai, L. Huang, Q. Guan, and L. L. Lai, "Decentralized finite control set model predictive control strategy of microgrids for unbalanced and harmonic power management," *IEEE Access*, vol. 8, pp. 202298–202311, 2020, doi: 10.1109/ACCESS.2020.3034947.

[4] R. Lasseter, "MicroGrids," in *Proc. IEEE Power Eng. Soc. Winter Meeting. Conf.*, vol. 1, Jan. 2002, pp. 305–308.

[5] J. Rocabert, A. Luna, F. Blaabjerg, and P. Rodríguez, "Control of power converters in AC microgrids," *IEEE Trans. Power Electron.*, vol. 27, no. 11, pp. 4734–4749, Nov. 2012.

[6] A. A. A. Radwan and Y. A. I. Mohamed, "Networked control and power management of AC/DC hybrid microgrids," *IEEE Syst. J.*, vol. 11, no. 3, pp. 1662–1673, Sep. 2017.

[7] J. Kim, J. M. Guerrero, P. Rodriguez, R. Teodorescu, and K. Nam, "Mode adaptive droop control with virtual output impedances for an inverter-based flexible AC microgrid," *IEEE Trans. Power Electron.*, vol. 26, no. 3, pp. 689–701, Mar. 2011.

[8] J. Lu, X. Liu, M. Savaghebi, X. Hou, and P. Wang, "Distributed event-triggered control for harmonic voltage compensation in islanded AC microgrids," *IEEE Trans. Smart Grid*, vol. 13, no. 6, pp. 4190–4201, Nov. 2022, doi: 10.1109/TSG.2022.3186284.

[9] G. Wang, X. Wang, and J. Lv, "An improved harmonic suppression control strategy for the hybrid microgrid bidirectional AC/DC converter," *IEEE Access*, vol. 8, pp. 220422–220436, 2020, doi: 10.1109/ACCESS.2020.3042572.

[10] R. Sinvula, K. M. Abo-Al-Ez, and M. T. Kahn, "Harmonic source detection methods: A systematic literature review," *IEEE Access*, vol. 7, pp. 74283–74299, 2019, doi: 10.1109/ACCESS.2019.2921149.

[11] N. Hazarika, J. Z. Chen, A. C. Tsoi, and A. Sergejew, "Wavelettransform," *Signal Process.*, vol. 59, no. 1, pp. 61–72, 1997.

[12] N. E. Huang, Z. Shen, S. R. Long, M. C. Wu, H. H. Shih, Q. Zheng, N.-C. Yen, C. C. Tung, and H. H. Liu, "The empirical mode decomposition and the Hilbert spectrum for nonlinear and non-stationary time series analysis," *Proc. Roy. Soc. London. Ser. A, Math., Phys. Eng. Sci.*, vol. 454, no. 1971, pp. 903–995, Mar. 1998.

[13] T. T. Nguyen, "Parametric harmonic analysis," *IEE Proc.-Gener., Transmiss. Distrib.*, vol. 144, no. 1, pp. 21–25, 1997.

[14] X. Wu, Y. Li, and H. Chen, "Programmable wavelet packet transform processor," *Electron. Lett.*, vol. 35, no. 6, p. 449, Mar. 1999.

[15] H. V. Young, Y.-C. Lin, and Y.-H. Wang, "On the memory cost of EMD algorithm," *IEEE Access*, vol. 10, pp. 114242–114251, 2022.

[16] L. Aswanuwath, W. Pannakkong, J. Buddhakulsomsiri, J. Karnjana, and V.-N. Huynh, "A hybrid model of VMD-EMD-FFT, similar days selection method, stepwise regression, and artificial neural network for daily electricity peak load forecasting," *Energies*, vol. 16, no. 4, p. 1860, Feb. 2023.

[17] X. Xi, P. Sun, C. Xing, S. Li, and X. Tian, "A parameter optimized variational mode decomposition method for harmonic and inter-harmonic detection," in *Proc. IEEE 12th Data Driven Control Learn. Syst. Conf. (DDCLS)*, May 2023, pp. 1877–1882.

[18] A. Sheng, L. Xie, Y. Zhou, Z. Wang, and Y. Liu, "A hybrid model based on complete ensemble empirical mode decomposition with adaptive noise, GRU network and whale optimization algorithm for wind power prediction," *IEEE Access*, vol. 11, pp. 62840–62854, 2023, doi: 10.1109/ACCESS.2023.3287319.

[19] H. Mahgoun, F. Chaari, and A. Felkaoui, "Detection of gear faults using variational mode decomposition (VMD)," *Mech. Ind.*, vol. 17, no. 2, p. 207, Feb. 2016.

[20] Y. Yue, L. Cao, B. Hang, and Z. Luo, "A swarm intelligence algorithm for routing recovery strategy in wireless sensor networks with mobile sink," *IEEE Access*, vol. 6, pp. 67434–67445, 2018, doi: 10.1109/ACCESS.2018.2879364.

[21] T. Zhang, Y. Qiao, J. Zhou, Z. Zhang, Y. Lu, and F. Su, "Spectral-efficient L/E-ACO-SCFDM-based dimmable visible light communication system," *IEEE Access*, vol. 7, pp. 10617–10626, 2019, doi: 10.1109/ACCESS.2019.2890881.

[22] M. T. Oakley, E. G. Richardson, H. Carr, and R. L. Johnston, "Protein structure optimization with a 'Lamarckian' ant colony algorithm," *IEEE/ACM Trans. Comput. Biol. Bioinf.*, vol. 10, no. 6, pp. 1548–1552, Nov. 2013, doi: 10.1109/TCBB.2013.125.

[23] M.-T. Pham, D. Zhang, and C. S. Koh, "Multi-guider and cross-searching approach in multi-objective particle swarm optimization for electromagnetic problems," *IEEE Trans. Magn.*, vol. 48, no. 2, pp. 539–542, Feb. 2012, doi: 10.1109/TMAG.2011.2173559.

[24] S. Zhou, X. Xu, Z. Xu, W. Chang, and Y. Xiao, "Fractional-order modeling and fuzzy clustering of improved artificial bee colony algorithms," *IEEE Trans. Ind. Informat.*, vol. 15, no. 11, pp. 5988–5998, Nov. 2019, doi: 10.1109/TII.2019.2936371.

[25] S. Mohanty, B. Subudhi, and P. K. Ray, "A new MPPT design using grey wolf optimization technique for photovoltaic system under partial shading conditions," *IEEE Trans. Sustain. Energy*, vol. 7, no. 1, pp. 181–188, Jan. 2016, doi: 10.1109/TSTE.2015.2482120.

[26] A. I. Sharaf and E.-S. F. Radwan, "An automated approach for developing a convolutional neural network using a modified firefly algorithm for image classification," in *Applications of Firefly Algorithm and its Variants*, 2020, p. 99.

[27] A. A. Heidari, S. Mirjalili, H. Faris, I. Aljarah, M. Mafarja, and H. Chen, "Harris hawks optimization: Algorithm and applications," *Future Gener. Comput. Syst.*, vol. 97, pp. 849–872, Aug. 2019, doi: 10.1016/j.future.2019.02.028.

[28] K. Dragomiretskiy and D. Zosso, "Variational mode decomposition," *IEEE Trans. Signal Process.*, vol. 62, no. 3, pp. 531–544, Feb. 2014.

[29] N. K. Sharma, S. R. Samantaray, and C. N. Bhende, "VMD-enabled current-based fast fault detection scheme for DC microgrid," *IEEE Syst. J.*, vol. 16, no. 1, pp. 933–944, Mar. 2022, doi: 10.1109/JSYST.2021.3057334.

[30] K. Anjaiah, P. K. Dash, R. Bisoi, and J. Divya, "Arc faults detection using VMD based DTEO in a PV-battery based DC microgrid," in *Proc. Int. Conf. Recent Adv. Mech. Eng. Res. Develop.*, 2023, p. 397.

[31] G. Rudolph, "Local convergence rates of simple evolutionary algorithms with Cauchy mutations," *IEEE Trans. Evol. Comput.*, vol. 1, no. 4, pp. 249–258, Nov. 1997, doi: 10.1109/4235.687885.

[32] D. Zhao, H. Yu, X. Fang, L. Tian, and P. Han, "A path planning method based on multi-objective Cauchy mutation cat swarm optimization algorithm for navigation system of intelligent patrol car," *IEEE Access*, vol. 8, pp. 151788–151803, 2020, doi: 10.1109/ACCESS.2020.3016565.

[33] S. Rahnamayan, H. R. Tizhoosh, and M. M. A. Salama, "Opposition-based differential evolution," *IEEE Trans. Evol. Comput.*, vol. 12, no. 1, pp. 64–79, Feb. 2008, doi: 10.1109/TEVC.2007.894200.

[34] V. Petridis, S. Kazarlis, and A. Bakirtzis, "Varying fitness functions in genetic algorithm constrained optimization: The cutting stock and unit commitment problems," *IEEE Trans. Syst. Man, Cybern. B, Cybern.*, vol. 28, no. 5, pp. 629–640, Oct. 1998, doi: 10.1109/3477.718514.

[35] F. Wang, C. Liu, W. Su, Z. Xue, Q. Han, and H. Li, "Combined failure diagnosis of slewing bearings based on MCKD-CEEMD-ApEn," *Shock Vibrat.*, vol. 2018, pp. 1–13, Apr. 2018.

[36] G. Tang and X. Wang, "Application of parameter-optimized variational mode decomposition in early fault diagnosis of rolling bearings," *J. Xi'an Jiaotong Univ.*, vol. 49, pp. 73–81, Jan. 2015.

[37] Y. Jiang, B. Tang, and S. Dong, "Application of parameter-optimized variational mode decomposition in early fault diagnosis of rolling bearings," *Chin. J. Sci. Instrum.*, vol. 31, pp. 56–60, Apr. 2010, doi: 10.19650/j.cnki.cjsi.2010.01.010.

[38] S. Das and B. Singh, "Coordinated control for performance enhancement of an islanded AC/DC microgrid with uninterrupted power and seamless transition capabilities," *IEEE Trans. Ind. Appl.*, vol. 58, no. 5, pp. 6676–6686, Sep. 2022.

[39] Y. Wang, W. Chen, and Z. Shen, "Modeling of litz wire winding AC resistance based on improved segmented equivalent circuit," *IEEE Trans. Power Electron.*, vol. 39, no. 1, pp. 1135–1149, Jan. 2024.

[40] E. G. Vera, C. A. Cañizares, M. Pirnia, T. P. Guedes, and J. D. M. Trujillo, "Two-stage stochastic optimization model for multi-microgrid planning," *IEEE Trans. Smart Grid*, vol. 14, no. 3, pp. 1723–1735, May 2023.

[41] Y. Zhong, J. Zhang, G. Li, and A. Liu, "Research on energy efficiency of supercapacitor energy storage system," in *Proc. Int. Conf. Power Syst. Technol.*, Oct. 2006, pp. 1–4, doi: 10.1109/ICPST.2006.321547.

[42] B. Saude, N. LaSart, J. Blair, and O. Beik, "Microgrid-based wind and solar power generation on moon and Mars," *IEEE Trans. Smart Grid*, vol. 14, no. 2, pp. 1329–1332, Mar. 2023, doi: 10.1109/TSG.2022.3210774.

[43] S. Sharma, B. K. Chauhan, and N. K. Saxena, "Artificial neural network grid-connected MPPT-based techniques for hybrid PV-WIND with battery energy storage system," *J. Inst. Eng. India, Ser. B*, vol. 104, no. 6, pp. 1217–1226, Dec. 2023.

[44] V. Nayanar, N. Kumaresan, and N. Ammasai Gounden, "A single-sensor-based MPPT controller for wind-driven induction generators supplying DC microgrid," *IEEE Trans. Power Electron.*, vol. 31, no. 2, pp. 1161–1172, Feb. 2016, doi: 10.1109/TPEL.2015.2420568.

[45] V. K. Dunna, K. P. B. Chandra, P. K. Rout, and B. K. Sahu, "Design and real-time validation of higher order sliding mode observer-based integral sliding mode MPPT control for a DC microgrid," *IEEE Can. J. Electr. Comput. Eng.*, vol. 45, no. 4, pp. 418–425, Fall. 2022, doi: 10.1109/ICJECE.2022.3211470.

[46] S. Shubhra and B. Singh, "Three-phase grid-interactive solar PV-battery microgrid control based on normalized gradient adaptive regularization factor neural filter," *IEEE Trans. Ind. Informat.*, vol. 16, no. 4, pp. 2301–2314, Apr. 2020, doi: 10.1109/TII.2019.2937561.

[47] F. A. Inthamoussou, J. Pegueroles-Queralt, and F. D. Bianchi, "Control of a supercapacitor energy storage system for microgrid applications," *IEEE Trans. Energy Convers.*, vol. 28, no. 3, pp. 690–697, Sep. 2013, doi: 10.1109/TEC.2013.2260752.

[48] S.-H. Choi, J.-S. Kim, J. Chae, J. Sim, and G.-W. Moon, "A nonlinear droop control for supercapacitor-hybrid uninterruptible power supplies in DC microgrids," in *Proc. 11th Int. Conf. Power Electron. ECCE Asia (ICPE-ECCE Asia)*, May 2023, pp. 1384–1389.

[49] B. Arras and Y. Swan, "IT formulae for gamma target: Mutual information and relative entropy," *IEEE Trans. Inf. Theory*, vol. 64, no. 2, pp. 1083–1091, Feb. 2018, doi: 10.1109/TIT.2017.2759279.

[50] T. E. Duncan, "Mutual information for stochastic signals and LÉvy processes," *IEEE Trans. Inf. Theory*, vol. 56, no. 1, pp. 18–24, Jan. 2010, doi: 10.1109/TIT.2009.2034800.

XINCHEN WANG was born in Xinyang, Henan, China, in 1999. She received the B.E. degree in electrical engineering and its automation from Huazhong University of Science and Technology, in 2021, where she is currently pursuing the master's degree.

She has two conference papers indexed in EI and IEEE, respectively, in the fields of harmonic detection and microgrid planning. Her research interests include power quality, multi-microgrid connection, and harmonic mitigation.

SHAORONG WANG was born in 1960. He received the B.E. degree in electrical engineering from Zhejiang University, Hangzhou, China, in 1984, the M.E. degree in electrical engineering from North China Electric Power University, Baoding, China, in 1990, and the Ph.D. degree in electrical engineering from Huazhong University of Science and Technology, Wuhan, China, in 2004. He is currently a Professor with Huazhong University of Science and Technology (HUST). His current research interests include smart grids, power system operation and control, wind power, and renewable energy.

JIAXUAN REN was born in Jinan, Shandong, China, in 1999. He received the B.E. degree in electrical engineering and its automation from North China Electric Power University, in 2022. He is currently pursuing the master's degree with Huazhong University of Science and Technology. He has two conference papers indexed in EI and IEEE, in the fields of intelligent operation and inspection of substations and harmonic coupling characteristics. His current research interest includes the power quality in power systems.

WEIWEI JING was born in 1981. He is currently a Senior Engineer and the Deputy Director of the Equipment Management Department, State Grid Jiangsu Electric Power Company Ltd. Specializing in electric grid development planning, production, and technical management for operations and maintenance. Moreover, he has successfully completed over ten scientific and technological projects for State Grid Corporation of China.

MINGMING SHI was born in 1986.

He is currently a Senior Engineer and the Deputy Director of the Distribution Network Technology Center, Electric Power Research Institute, State Grid Jiangsu Electric Power Company Ltd. In recent years, he has focused on researching power quality testing and analysis, along with exploring the application of power electronic technology in the power grid. He has published a total of 15 articles indexed in SCI and EI databases.

XIAN ZHENG was born in 1995. She received the Ph.D. degree from Sichuan University.

She joined the Electric Power Research Institute, State Grid Jiangsu Electric Power Company Ltd., in 2021. She is currently dedicated to research in the field of power quality and harmonic analysis. She has authored over ten articles published in reputable journals and presented three papers at major international academic conferences, including CIRED and ICHQP.